Tidal turbine wake characterization by vessel-mounted ADCP data analysis

Patxi Garcia-Novo, Masako Inubuse, Masakatsu Terazaki, Hiroshi Matsuo, Philip Archer, Katsuhiro Henzan, Yusaku Kyozuka, and Daisaku Sakaguchi

Abstract—**Wakes generated downstream turbines are one of the key points to be considered for tidal stream energy farm layout design. Distance between consecutive turbines must be optimized considering available resource spatial distribution and the current velocity reduction caused by upstream turbines. Tidal turbine wake characteristics have been analyzed experimentally and numerically, however, there is still a lack of studies presenting data measured in the wake of large-size turbines in tidal sites. In this paper, the wake generated downstream of a SIMEC Atlantis Energy 0.5 MW turbine in Naru Strait (Nagasaki Prefecture, Japan) is analyzed using data measured with a vessel-mounted ADCP (Acoustic Doppler Current Profiler). This analysis is based on the comparison between data measured before turbine installation (September 2020) and during turbine operation (March 2021 and May 2021). Results show a velocity deficit with respect to current conditions without energy extraction even at a distance of 180 m (10 rotor diameters) from the turbine. In the vertical direction, the largest impact was found at the height corresponding with the center of the rotor. Quantitatively, the percentual velocity deficit in the main wake decreased from approximately 43% in the near wake (2D-3D) to 16% at a distance of 13D, however this results are highly dependent on the density of measured data, thus should be confirmed in future works using bottom-mounted ADCPs.**

Index Terms—**Tidal energy, Turbine, Wake, Vessel-mounted, ADCP**

I. Introduction

DUE to the growing concern about climate change in the last decades, national governments are developing decarbonization plans for the first half of this century. This process will imply an increase in the electric power demand, which is expected to be covered by renewable energy sources [1]. Among these, tidal stream energy is one of the most promising conversion technologies. Its predictability and periodicity are two great advantages both for large-scale grids, where it can contribute to grid stabilization [2], and microgrids in remote areas, where it can reduce the total cost of the system due to its good adaptability to low-term energy storage technologies [1].

To date, MW-scale tidal stream energy turbines have been tested in demonstration and pre-commercial projects. In the Pentland Firth (Orkney Islands, Scotland), four 1.5 MW turbines have been simultaneously operating, reaching a maximum monthly export power of 1.4 GWh [3]. In Naru Strait (Goto Islands, Japan) [4], a 0.5 MW turbine was operating for 10 months with an availability higher than 96%. With these first projects providing successful results, the next step to commercialization is the construction and operation of tidal arrays with a larger number of turbines. In this regard, the installed capacity in the Pentland Firth is planned to increase from 6 MW to 86 MW by 2026 [3].

One of the main issues tidal stream energy technology has to face in this last step to commercialization is the high spatial variability of the resource. As an example, 41.4% of total available resource in Naru Strait (approx. dimensions 16 km^2) is concentrated in 2.5 km^2 [5]. Thus, to reduce the cost of tidal stream energy, an exhaustive optimization work to maximize the number of turbines installed in these narrow areas while mitigating the power losses due to the wakes generated by upstream turbines is crucial.

Several works have been published concerning the characterization and prediction of wakes downstream tidal turbines based on experimental data. Stallard et al [6] characterized the wake generated by a horizontal-axis turbine (HAT) rotor with a Tip Speed Ratio (TSR) of 4.7 and found the maximum velocity deficit around the rotation axis. By contrast, in tests presented by Chen [7] and Tedds [8] with other HATs with different TSR (3.53 and 6.15 respectively), the largest velocity deficit was observed at the blade tips. Atcheson et al [9] measured the velocity deficit 5D (5 diameters) downstream a larger rotor (1.5 m). They concluded that although the velocity deficit was independent of the input current velocity, this had an impact on the turbulence intensity measured downstream. The impact of

This work was supported by the Ministry of Environment of Japan under the Tidal Power Generation Technology Demonstration Project of Goto, Nagasaki.

P. G. N. Author is with the Graduate School of Engineering, Nagasaki University, 1-14 Bunkyo-machi, Nagasaki, 852-851 Japan (e-mail: patxi@nagasaki-u.ac.jp).

M. I. Author is with Seibu Environmental Research Co., Ltd., 26-1 Mikawachishinmachi, Sasebo, Nagasaki Prefecture, 859-3153 Japan (e-mail: inubuse@serc.jp).

M. T. Author is with Kyuden Mirai Energy Co., Inc., 3-2-23 Yakuin, Chuo-ku, Fukuoka, 810-0022 Japan (e-mail: masakatsu.terazaki@q-mirai.co.jp).

H. M. Author is with the Nagasaki Ocean Academy, 852-851, Bunkyo-machi, Nagasaki, Japan (e-mail: matsuo@namicpa.com).

P. A. Author is with Proteus Marine Renewables Ltd, UK (e-mail: p.archer@proteusmr.com).

K. H. Author is with Kyuden Mirai Energy Co., Inc., 3-2-23 Yakuin, Chuo-ku, Fukuoka, 810-0022 Japan (e-mail: katsuhiro.henzan@q-mirai.co.jp).

Y. K. Author is with the Organization for Marine Science and Technology, Nagasaki University, 1-14 Bunkyo-machi, Nagasaki, 852-851 Japan (e-mail: kyozuka@nagasaki-u.ac.jp).

D. S. Author is with the Graduate School of Engineering, Nagasaki University, 1-14 Bunkyo-machi, Nagasaki, 852-851 Japan (e-mail: daisaku@nagasaki-u.ac.jp).

Digital Object Identifier:
https://doi.org/10.36688/ewtec-2023-296

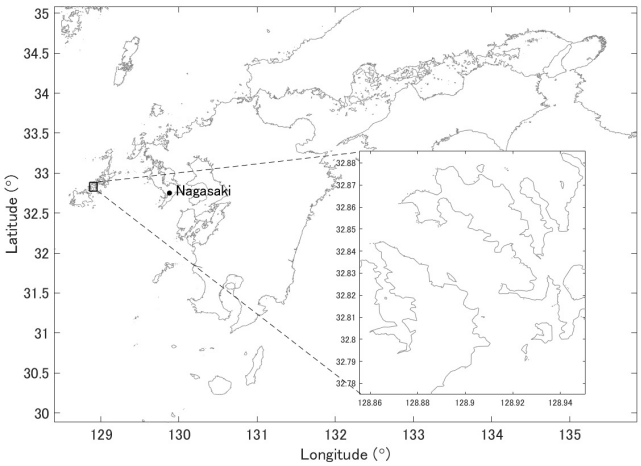

Fig. 1. Location map of Goto Islands and Naru Strait.

the turbulence conditions of the upstream flow on the wake generated downstream was evaluated by Mycek et al [10]., concluding that larger turbulence intensities lead to faster wake recovery.

However, the characterization of wakes generated by MW-scale turbines in a tidal site has not been addressed yet. In this paper, an analysis of the velocity deficit in the wake generated by an 18 m rotor diameter, 500 kW turbine installed in Naru Strait is presented. This analysis is based on the comparison of data measured with a vessel-mounted ADCP (Acoustic Doppler Current Profiler) before (November 2020) and after (March 2021 and May 2021) turbine installation.

II. Methods

A. Area of study

The data presented in this study was measured in the wake of a SIMEC Atlantis turbine installed in Naru Strait, Nagasaki Prefecture, Japan (see Fig 1). Naru Strait is one of the main four channels in the Goto Islands. It is located between Hisaka Island (west) and Naru Island (east) and its approximate dimensions are 7 km in length and 2 km in width, with a narrowing of 1 km in width in front of Kagaribizaki Cape. Depth in the central channel of Naru Strait ranges between 35 m and 50 m. The tides in this area are mixed semidiurnal tides and, according to data measured by a tidal station in Fukue Island (approx 15 km from the test site), the maximum tidal range is approximately 3 m. Despite this relatively low tidal range, due to its narrowness and shallowness strong tidal currents are generated in this channel. Maximum current velocities higher than 3 m/s have been observed [11], with the main current direction being SE-NW during flood tides and vice versa during ebb tides.

The turbine was installed at [32°49′4.3” N, 128°54′40.4” E], where the averaged depth is approximately 40 m. According to data measured by a Signature 500 ADCP at 74 m from the turbine installation point [32°49′6.6” N, 128°54′37.8” E] from October to December 2016 with a sampling frequency of 2 Hz the 5-min vertical averaged maximum current velocities for flood and ebb tides are 2.84 m/s and 3.00 m/s respectively. The flow direction is presented in the hodograph in Fig 2, which shows a slight asymmetry between flood and ebb tides. During flood tides, the main direction forms an angle of 29.55 degrees with the North, whereas with ebb tides the angle formed with the South is 9.27 degrees.

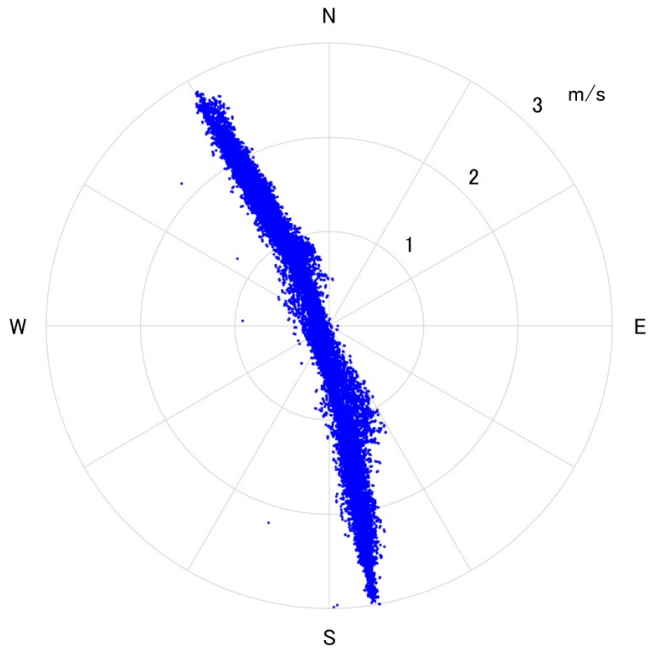

Fig. 2. Hodograph of vertical averaged current velocity at 74 m from the turbine installation point.

Data from this ADCP was also used to calculate turbulence intensity (TI) values for every 5-min period by Eq 1.

$$TI = \frac{\sigma_V}{\bar{V}} \tag{1}$$

where V is the current velocity. Results for TI and mean current velocity for every 5-min period are presented in Fig 3. To avoid the unrepresentative high TI in slack tides due to the very low values in the denominator, only flow conditions with vertical averaged current velocities over 1 m/s (corresponding with a typical cut-in speed for MW-sized turbines) are plotted.

Besides the increase of TI with depth due to the effect of bottom friction, a clear correlation with current velocity was observed, from an average of 0.1206 for current velocity of 1 m/s to 0.062 for 3 m/s flows at the rotor center height.

The first option considered for data measurement for the characterization of the wake generated downstream of the turbine was measuring current velocity with a bottom-fixed ADCP with a minimum sampling frequency of 2 Hz in the middle wake (5 to 10 diameters from the rotor) during approximately two months (from one month before to one month after turbine deployment). Thus, the impact of energy conversion on flow conditions could be characterized by comparing data measured before and after turbine installation. However, this could not be done due to the depth conditions of the site, since works involving divers were limited to areas with depths lower than

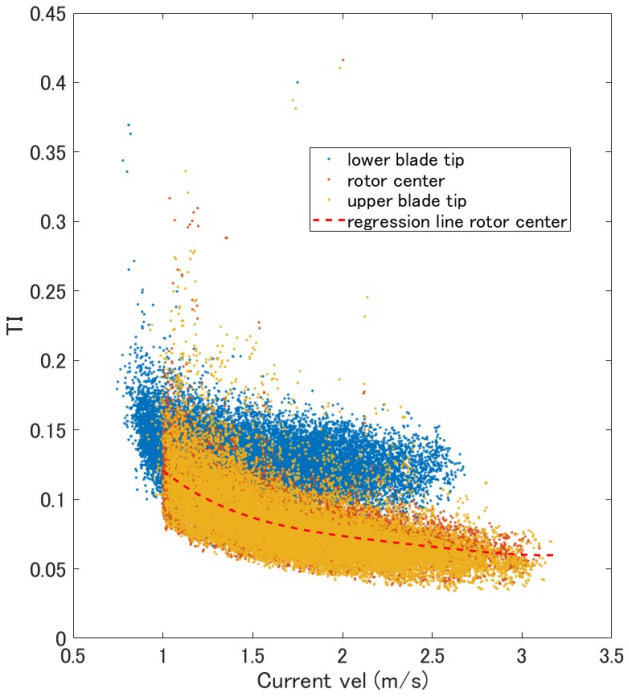

Fig. 3. Turbulence Intensity vs current velocity at the lower blade tip, rotor center and upper blade tip depths measured at 74 m from the turbine installation point.

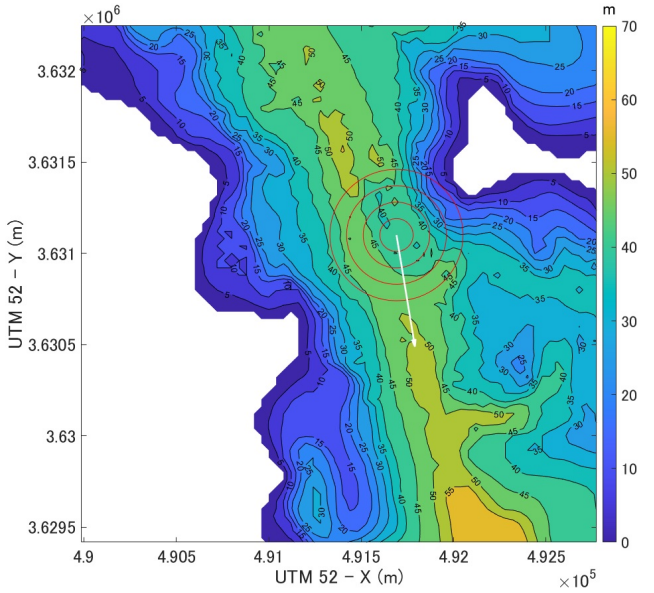

Fig. 4. Bathymetry map of Naru Strait. Concentric circles represent distances of 5D, 10D, 15D and 20D from the turbine. White arrow represents the main current direction during ebb tides at 74 m from the turbine installation point.

Fig. 5. ADCP-vessel attachment system.

40 m. Fig 4 shows a bathymetry map of the area surrounding the turbine installation point, as well as four concentric circles representing distances of 5D, 10D, 15D, and 20D from the turbine (red) and the main vertical-averaged flow direction (white arrow) during ebb tide in the turbine installation point. As shown in this map, in the area where the main wake is expected a location shallow enough to ensure a safe bottom-mounted ADCP installation could not be found. For this reason, current velocities in the area of the wake generated by the tidal turbine were measured with a vessel-mounted ADCP.

The ADCP used was an RDI WorkHorse 600 kHz. It was set to measure current velocity data in 42 vertical layers, 1 m width each. The distance of the center of these layers to the sea surface differed. In November 2020 and May 2021, current velocity data at a distance of 3.48 m, 4.48,... and 44.48 m from the surface was obtained. In March 2021, data was measured at 1 m intervals from 3.83 m and 44.83 m. The ADCP was coupled with a GPS system which provided the position of the ADCP for every sampling time. A picture of the attachment system of the ADCP to the vessel is shown in Fig 5.

B. Vessel routes

Current velocity conditions in the downstream area were measured with the vessel-mounted ADCP before and after turbine installation to compare data with and without tidal stream energy conversion. During the demonstration project in 2021, the turbine did not have a yaw system and only generated power during ebb tides. Thus, the measuring work focused on the area southeast of the tidal turbine.

The first work was carried out on November 15, 2020, from 9:58AM to 1:23PM, two months before turbine installation, whereas the second fieldwork was done on March 14, 2021, from 10:48AM to 2:31PM, two months after the turbine installation. The area covered in these two cases is marked in blue in Fig 6, and the routes followed by the vessel in November 2020 and March 2021 are shown in Fig 7 and Fig 8 respectively. In both cases, the vessel followed straight lines perpendicular to the main flow direction at the turbine position during ebb tide, with a distance between two consecutive lines of 2D (36 m), starting from NorthWest (near the turbine) to SouthEast. Additionally, when this perpendicular scan ended, the vessel moved back to the NorthWest following the line of the expected wake to start again the same procedure.

The third fieldwork focused on the area where the turbine impact was found more significant when comparing the current velocities measured in November

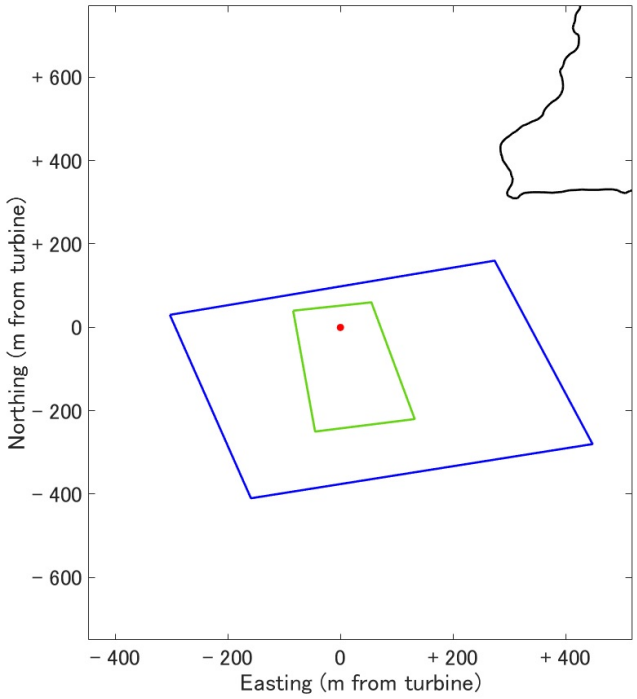

Fig. 6. Areas covered in November 2020 (blue), March 2021 (blue) and May 2021 (green). Turbine position is marked with a red dot.

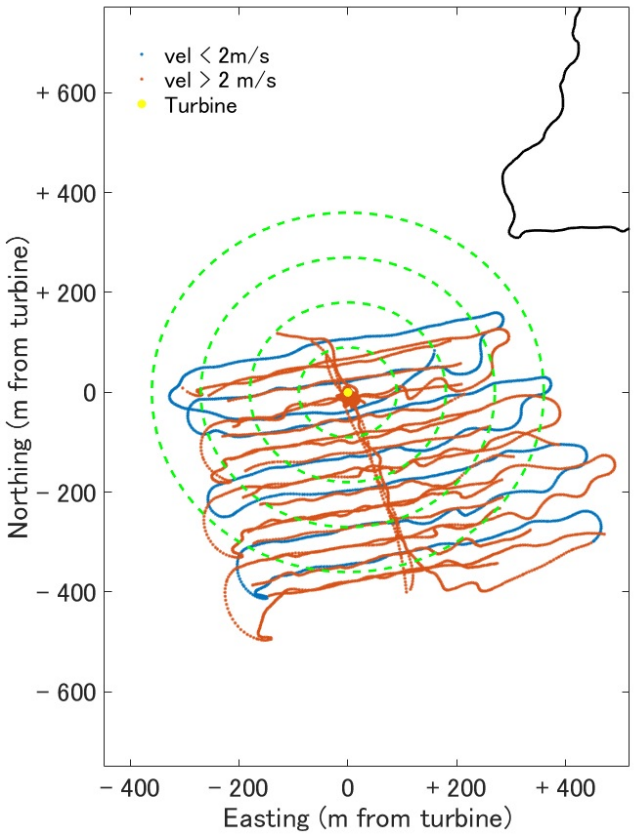

Fig. 7. Vessel route in November 2020 fieldwork. Blue dots represent positions of data measured when current velocity in the turbine position is higher than 1 m/s and lower than 2 m/s. Red dots represent positions of data measured when current velocity in the turbine position is higher than 2 m/s.

2020 and March 2021. Thus, works done on May 29, 2021, from 11:52AM to 3:09PM focused on the area

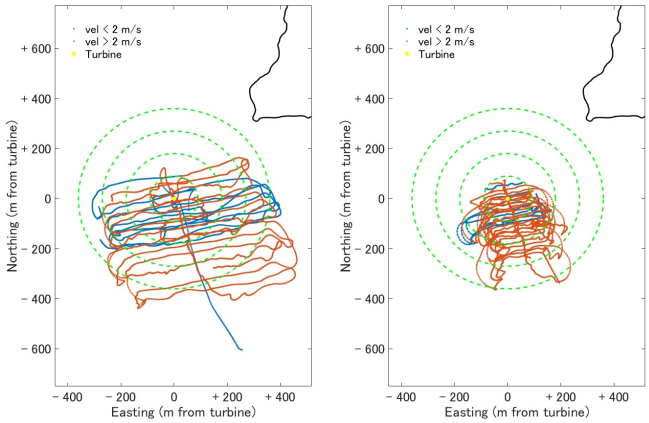

Fig. 8. Vessel route in March 2021 (left) and May 2021 (right) fieldworks. Blue dots represent positions of data measured when current velocity in the turbine position is lower than 2 m/s. Red dots represent positions of data measured when current velocity in the turbine position is higher than 2 m/s.

TABLE I
FIELDWORKS SUMMARY

Fielwork	Date	Time	Operating turbine
1	2020/11/15	09:58 - 13:23	NO
2	2021/03/14	10:48 - 14:31	YES
3	2021/05/29	11:52 - 15:09	YES

squared in green in Fig 6 and the distance between two consecutive lines perpendicular to the main flow direction was reduced to 1D. For the three fieldworks, the vessel moved with a speed between 2 and 4 knots in the lines perpendicular to the main flow direction and at 0.5 knots when following the main wake from SouthEast to NorthWest.

Current velocity conditions of the flow upstream of the turbine during the measurements done after turbine installation were obtained from data measured by an ADCP attached to the nacelle. For the November 2020 fieldwork, current velocity at the turbine location was estimated by harmonic analysis of the data measured by this ADCP. Dates and times of the three measuring works are presented in Table I.

C. Data treatment

In experimental works where current velocity can be kept constant through space, turbine impact on the velocity conditions downstream is characterized by means of a dimensionless parameter calculated by dividing the current velocity downstream turbine by the current velocity upstream turbine. However, due to the high spatial variability of current velocity, this method cannot be applied to a field tidal site. An alternative for treating field-measured data is comparing data measured before turbine installation and during turbine operation. However, with the data presented in this study, a direct comparison between the three datasets would require the vessel to be at the same tide moment and at the same position before and after installation. This is unfeasible due to the difficulties in predicting tidal currents in such an accurate way and the technical impossibility to follow an exact route

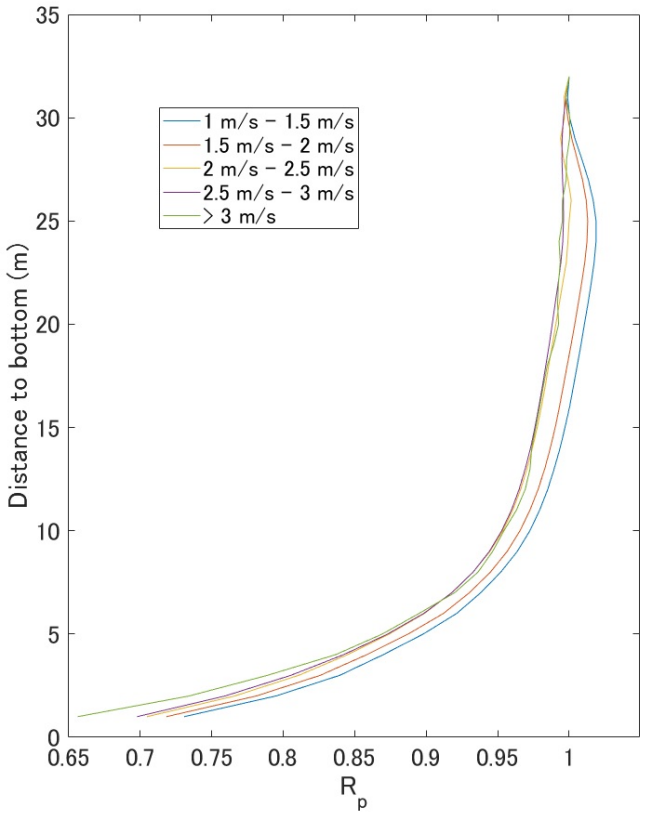

Fig. 9. Averaged R_p measured at 74 m from the turbine installation point for vertical averaged current velocities between 1 m/s and 1.5 m/s, 1.5 m/s and 2 m/s, 2 m/s and 2.5 m/s, 2 m/s and 3 m/s, and higher than 3 m/s.

with the vessel. To solve this issue, a profile ratio R_p was calculated for every 42-layers current velocity dataset by dividing the current velocity measured at every layer by the current velocity measured at the shallowest layer (Eq 2).

$$R_p = \frac{v_i}{v_1} \tag{2}$$

where i is the layer number (counting from surface to bottom) and v_1 is the shallowest measured layer. Results for R_p are interpolated to a structured 1m x 1m x 1m 3D mesh for easier comparison between the three datasets. Then, assuming that the velocity profile shape at one location does not change over time, the impact of tidal stream energy exploitation on the current velocity for every position within the measured area is parameterized with a variation ratio (R_v) calculated by dividing R_p before turbine installation by R_p after turbine installation (Eq 3).

$$R_v = \frac{R_{p_{with\,turbine}}}{R_{p_{without\,turbine}}} \tag{3}$$

A possible source of error using this method is the variability of the vertical profile shape with current velocity. To confirm this issue, data measured by the bottom-fixed ADCP in 2016 at the turbine installation point was separated into five different groups depending on the vertical averaged velocity (between 1 m/s and 1.5 m/s, between 1.5 m/s and 2 m/s, between 2 m/s and 2.5 m/s, between 2.5 m/s and 3 m/s, and higher than 3 m/s). Average vertical profiles of R_p for each of these groups presented in Fig 9 show that, although similar shapes are observed for the five cases, slight differences could be found between profiles with vertical averaged current velocities lower than 2 m/s and higher than 2 m/s. For this reason, the data treatment described in this section was applied separately for both groups. Also, this separation allows an evaluation of the impact of the upstream flow conditions on the generated wake.

A mapping of the data corresponding to each of these groups for data measured in November 2020, March 2021 and May 2021 are presented in Fig 7 and Fig 8. Locations of data measured when current velocity at the turbine position is lower than 2 m/s are represented in blue and locations of data measured under current velocities larger than 2 m/s at the turbine position are represented in red. Also, the turbine position is shown in yellow, and circles representing distances of 5D, 10D, 15D, and 20D from the turbine are marked with green broken lines. During the November 2020 fieldwork, the area covered under both current velocity conditions was similar. However, for the fieldwork done after turbine installation, the data available for the first group (vel $<$ 2 m/s) covers a smaller area (up to 10D from turbine in March and 5D from turbine in May).

III. Results

Results of R_p obtained from the treatment of data measured at 26 m from the surface (corresponding with the rotor hub height) in lines perpendicular to the main flow direction in March 2021 from 12:00 to 13:47 are shown in Fig 10. Lines represented in this graph correspond to distances from approximately 1D to 21D, at 2D intervals. As for the previous maps, concentric circumferences at 5D, 10D, 15D, and 20D are plotted for reference. A velocity deficit in the wake of the turbine (black dot) is observed, with a significant decrease in the R_p values from 0.8-1 in both sides of the wake to 0.2-0.5 downstream of the turbine. Data represented in this map gives also an idea of the distance needed for wake recovery. While R_p values between 0.2 and 0.5 are found from the turbine to a distance of 5D, this increases to approximately 0.7 near 10D, and reaches values between 0.8 and 1.0 from 15D.

The impact of energy conversion on the tidal currents could be confirmed also with data measured when the vessel was following the line corresponding with the expected wake from SouthEast to NorthWest. This impact is clear in the vertical profiles for R_v at 1D, 2D, 3D, 4D, 5D, 6D and 9D from the turbine in Fig 11. Lower values of R_v are observed in the vertical area covered by the rotor, from 17 m to 35 m from the surface, with peaks near the depth corresponding with the rotor hub position. However, conclusions regarding velocity deficit or wake recovery cannot be extracted from these profiles due to the difficulties of the vessel to drive straight following the main wake direction.

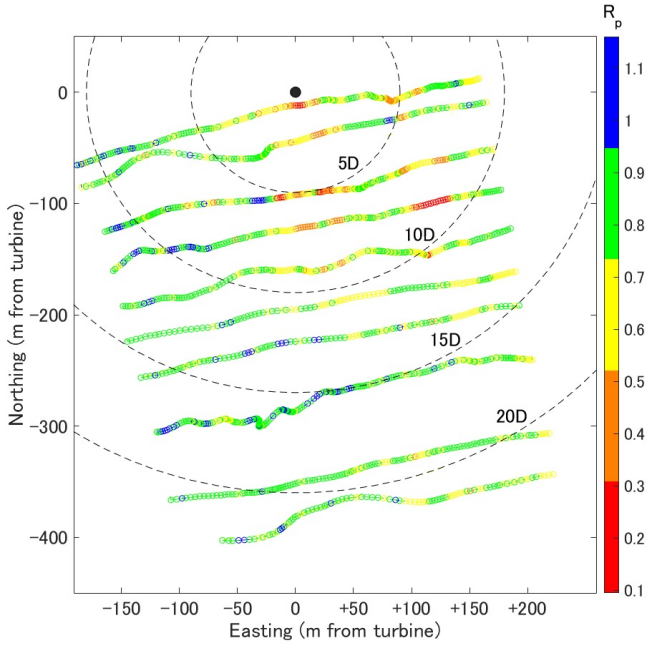

Fig. 10. R_p at the rotor hub depth measured in lines perpendicular to the main current direction.

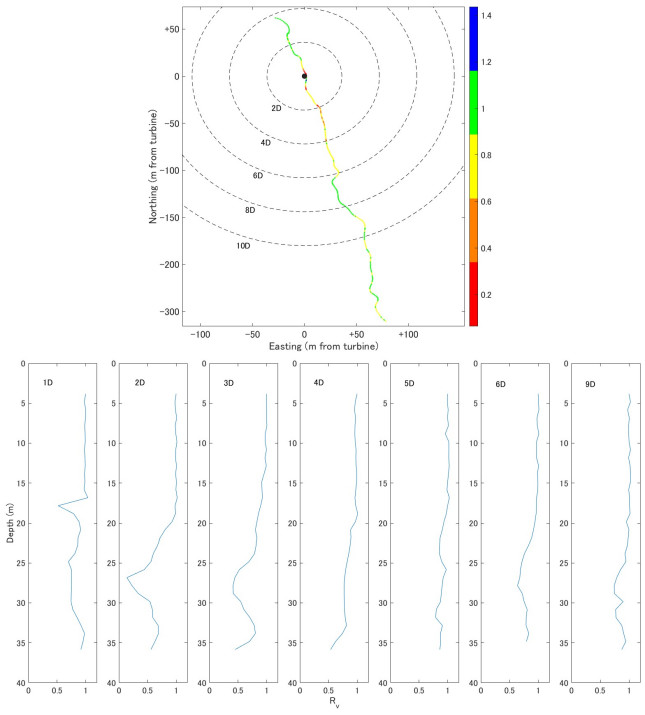

Fig. 11. R_p at the rotor hub depth measured in the line parallel to the main current direction (up) and R_p profiles at 1D, 2D, 3D, 4D, 5D, and 9D from the turbine (down)

A. Comparison of flow conditions before and after energy conversion

In this section, current conditions before and after turbine installation are compared based on the results of the interpolation of the data measured in November 2020, March 2021 and May 2021 to a regular mesh.

Results of this comparison using data measured with current velocities between 1 m/s and 2 m/s in the upstream flow are presented in Fig 12 for a water depth of

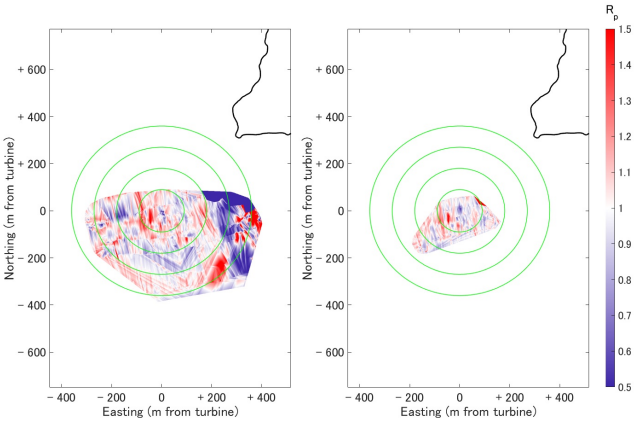

Fig. 12. R_v at the rotor hub depth using data measured in November 2020 and March 2021 (left) and in November 2020 and May 2021 (right) when the current velocity in the turbine position is higher than 1 m/s and lower than 2 m/s.

26 m from the surface, corresponding with the turbine hub height, where the velocity deficit is expected to be higher according to the R_p profiles presented in Fig 11. Likewise, Fig 13 and Fig 14 show R_v results at this same depth using data measured when current velocity at the turbine location was between 2 m/s and 3 m/s. Areas where the operating turbine causes deficit and increase in current velocity are presented in blue and red respectively. These maps show the weaknesses of the method used for the parameterization of the turbine impact on the current velocity. First, the area mapped is limited by the available data. Second, the results of interpolation to the structured mesh are also affected by the spatial density of measured data. In the map comparing November 2020 and March 2021 datasets (Fig 13), although a blue area of velocity deficit appears downstream of the turbine in the direction of the flow, this is broken with some white (or even red) small regions due to the lack of data (i.e. 2D or 9D). On the other hand, in the map generated with the comparison of data measured in November 2020 and May 2021 (Fig 14) the interruptions in the blue wake are less and smaller, with only a small white region in the area adjacent to the turbine ($< 1D$).

This issue made impossible the comparison of wake conditions for different upstream flows due to the narrower covered area and the lower data spatial density when current velocities at the turbine installation point were between 1 m/s and 2 m/s. For this reason, further results presented in this section analyze only the impact of energy conversion when current velocity at the turbine location is between 2 m/s and 3 m/s.

In the horizontal direction, Fig 13 and Fig 14 clearly show a velocity deficit in the main wake from the turbine location to a distance of 10D.

Furthermore, the variability of R_v with depth is represented in Fig 15. These profiles are obtained from the comparison of interpolated data from November 2020 and May 2021, since data measured during this second fieldwork has a higher spatial density. In this graph, two red broken lines corresponding with the rotor's lower and upper tip and one green broken line in $R_v = 1$ are added for reference. The velocity deficit

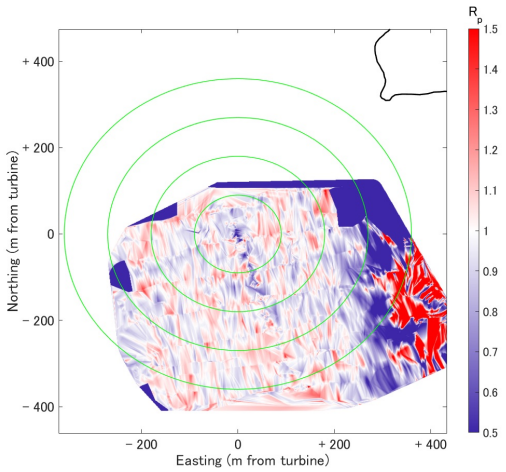

Fig. 13. R_v at the rotor hub depth using data measured in November 2020 and March 2021 when the current velocity in the turbine position is higher than 2 m/s.

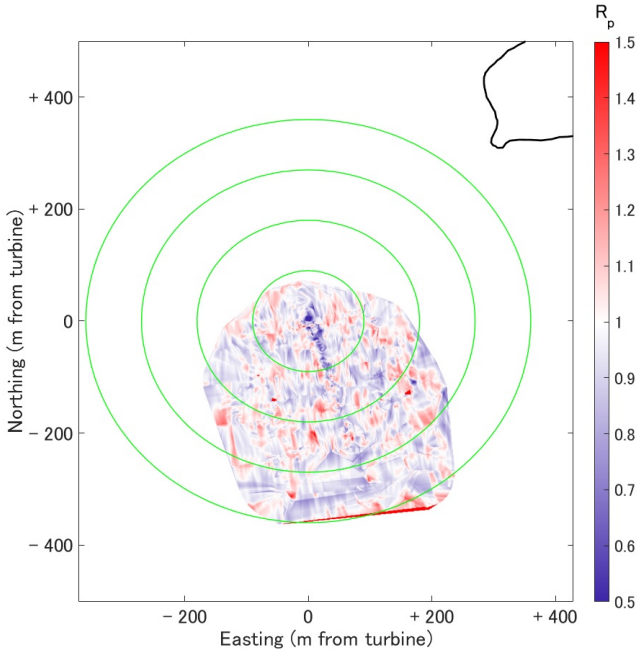

Fig. 14. R_v at the rotor hub depth using data measured in November 2020 and May 2021 when the current velocity in the turbine position is higher than 2 m/s.

in the turbine wake is clear from 1D to 5D, with its peak at the center of the rotor. Quantitatively, the minimum values for R_v for 1D, 2D, 3D, 4D, and 5D are 0.71, 0.57, 0.56, 0.73, and 0.68 respectively.

From 6D, there is not a clear trend in the profiles. Whereas at 8D, 9D, 13D, and 14D a reduction in current velocity was observed (minimum R_v=0.76, 0.73, 0.84, and 0.72 respectively), other profiles are nearly constant with depth and close to 1, thus meaning a negligible impact of the tidal turbine on the current velocity conditions at that point. Furthermore, at 6D and 12D from the turbine, a notable increase in current velocity is observed at the rotor's hub height (maximum R_v=1.23 and 1.38 respectively).

The variability of R_v profile shapes from 6D from the turbine might be due to the lower data density, which increases the interpolation error. Also, for this

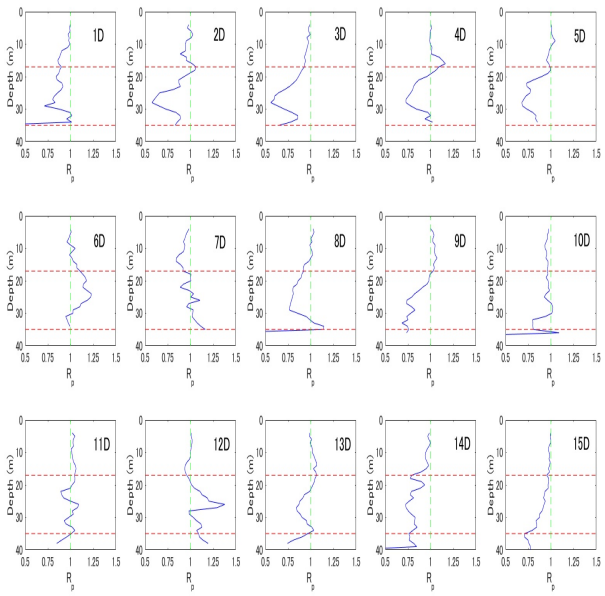

Fig. 15. R_v profiles from 1D to 15D from the turbine, at 1D intervals. Red broken lines represent rotor's lower and upper tip.

analysis, it was considered that the wake followed a straight line with the main direction of the flow upstream of the turbine. Thus, slight deviations in this direction will cause the points selected for the R_v profile representation might not to fall on the main wake, but at one of its sides, where an increase in current velocity is expected [12].

IV. Discussion

Due to the notable temporal [11] and spatial (see Fig 10) variability of current conditions in tidal energy sites, a complete and exhaustive characterization of the wake generated downstream the turbine using data measured on-site would require measuring data in a grid of points dense enough in the wake area for a period of time long enough to cover tide temporal fluctuation. This is technically and economically unfeasible, thus available data must be treated following processing methods that have an associated error. The reliability of the results obtained with the data analysis described in this paper is discussed in this section.

Qualitatively, the data measured with the vessel-mounted ADCP showed a clear velocity deficit area in the wake generated downstream of the turbine, with still an impact at a distance of 10D. This is reflected in the representation of data measured in Fig 10 and Fig 11, as well as in the mapping of R_v obtained by spatial interpolation. On the contrary, quantitative conclusions cannot be extracted from this data due to the limitations of the methods used for the data treatment. Results from interpolation to the regular mesh are highly dependent on the spatial density of measured data. In this regard, although in the May 2021 fieldwork, most data was measured in the area close to the main wake, which should reduce the interpolation-related error, the other comparative element (November 2021) results from the interpolation of data with lower spatial density, which affects to the reliability of the final results.

Besides the error associated with the interpolation, the assumption that the velocity profile shape does not change in time is another possible source of error. Although similar profiles were confirmed for the turbine installation point for vertical-averaged velocities over 2 m/s, the situation might be different for other locations covered during the three fieldworks. Examples of velocity profile shapes varying with current velocity are available in the literature for other locations in the Goto Islands [13].

Despite these limitations, results presented in this paper are of great value since these can be used for the validation of numerical models, which later can be used to simulate different flow conditions and turbine characteristics to evaluate their impact on the generated wake.

For future measurements of the velocity deficit in the wake generated by tidal turbines, we suggest that vessel-mounted ADCP data be complemented with bottom-fixed ADCP measurements. Whereas the former provides information for a wide area so that the length and direction of the wake can be confirmed, the second gives quantitative information that can be used for the validation of numerical models. Also, bottom-fixed ADCPs can provide data for longer time periods, so that the influence of upstream flow conditions on the wake can be analyzed. Furthermore, treatment of this data would give information regarding other important wake-defining characteristics, such as turbulence-related parameters. Other options such as the attachment of ADCPs to ROVs (Remotely Operated Vehicles) [14], which can offer advantages associated with both vessel-mounted and bottom-fixed ADCPs, should be also considered in the future.

V. Conclusion

This paper presents a new analysis method for field data measured by a vessel-mounted ADCP in the wake of tidal turbines. To allow comparison between data measured before turbine installation and during turbine operation, data is pretreated first by calculating a profile-defining parameter for every measured point and then by interpolating it to a regular three-dimensional mesh.

Qualitatively, the impact of the turbine on the current velocity downstream could be confirmed with this data. Velocity deficit caused by the turbine could be observed from the turbine to a distance of 10D, with the strongest impact in the depth corresponding with the rotor's hub. However, the reliability of the quantitative analysis for the velocity deficit and wake recovery is limited by the data processing methods (interpolation to regular mesh) and assumptions (R_v profile shape independent of current velocity).

The results presented in this paper are of great value for the validation of numerical models simulating the impact of tidal turbines on the current velocity of the downstream flow in tidal energy sites.

Acknowledgement

This work was supported by the Ministry of Environment of Japan under the Tidal Power Generation Technology Demonstration Project of Goto, Nagasaki.

References

[1] D. Coles, B. Wray, R. Stevens, S. Crawford, S. Pennock, and J. Miles, "Impacts of tidal stream power on energy system security: An isle of wight case study," *Applied Energy*, vol. 334, p. 120686, 2023. [Online]. Available: https://www.sciencedirect.com/science/article/pii/S0306261923000508

[2] P. Garcia Novo and Y. Kyozuka, "Tidal stream energy as a potential continuous power producer: A case study for west japan," *Energy Conversion and Management*, vol. 245, p. 114533, 2021. [Online]. Available: https://www.sciencedirect.com/science/article/pii/S0196890421007093

[3] "Simec atlantis energy," https://saerenewables.com/tidal-stream/meygen/, accessed: 2023-05-23.

[4] "Simec atlantis energy," https://saerenewables.com/sae-achieves-another-tidal-milestone-in-japan/, accessed: 2023-05-23.

[5] P. Garcia Novo, Y. Kyozuka, and M. H, "Tidal energy resource assessment map for nagasaki prefecture," in *Proceedings of Grand Renewable Energy 2018*, vol. 1, 2018, p. 237.

[6] T. Stallard, T. Collings, T. Feng, and J. Whelan, "Interactions between tidal turbine wakes: experimental study of a group of three-bladed rotors," *Philosophical Transactions of the Royal Society A*, vol. 371, p. 20120159, 2013.

[7] Y. Chen, B. Lin, J. Lin, and S. Wang, "Experimental study of wake structure behind a horizontal axis tidal stream turbine," *Applied Energy*, vol. 196, pp. 82–96, 2017. [Online]. Available: https://www.sciencedirect.com/science/article/pii/S0306261917303720

[8] S. Tedds, I. Owen, and R. Poole, "Near-wake characteristics of a model horizontal axis tidal stream turbine," *Renewable Energy*, vol. 63, pp. 222–235, 2014. [Online]. Available: https://www.sciencedirect.com/science/article/pii/S0960148113004783

[9] M. Atcheson, P. MacKinnon, and B. Elsaesser, "A large scale model experimental study of a tidal turbine in uniform steady flow," *Ocean Engineering*, vol. 110, pp. 51–61, 2015. [Online]. Available: https://www.sciencedirect.com/science/article/pii/S0029801815005326

[10] P. Mycek, B. Gaurier, G. Germain, G. Pinon, and E. Rivoalen, "Experimental study of the turbulence intensity effects on marine current turbines behaviour. part i: One single turbine," *Renewable Energy*, vol. 66, pp. 729–746, 2014. [Online]. Available: https://www.sciencedirect.com/science/article/pii/S096014811400007X

[11] P. Garcia Novo and Y. Kyozuka, "Validation of a turbulence numerical 3d model for an open channel with strong tidal currents," *Renewable Energy*, vol. 162, pp. 993–1004, 2020. [Online]. Available: https://www.sciencedirect.com/science/article/pii/S0960148120312726

[12] S. Salunkhe, O. El Fajri, S. Bhushan, D. Thompson, D. O'Doherty, T. O'Doherty, and A. Mason-Jones, "Validation of tidal stream turbine wake predictions and analysis of wake recovery mechanism," *Journal of Marine Science and Engineering*, vol. 7, no. 10, 2019. [Online]. Available: https://www.mdpi.com/2077-1312/7/10/362

[13] P. Garcia Novo and Y. Kyozuka, "Field measurement and numerical study of tidal current turbulence intensity in the kobe strait of the goto islands, nagasaki prefecture," *Journal of Marine Science and Technology*, vol. 22, pp. 335–350, 2017. [Online]. Available: https://doi.org/10.1007/s00773-016-0414-x

[14] M. Guerra, A. E. Hay, R. Karsten, G. Trowse, and R. A. Cheel, "Turbulent flow mapping in a high-flow tidal channel using mobile acoustic doppler current profilers," *Renewable Energy*, vol. 177, pp. 759–772, 2021. [Online]. Available: https://www.sciencedirect.com/science/article/pii/S0960148121008168